How to cite: *Angew. Chem. Int. Ed.* **2025**, *64*, e202405125
doi.org/10.1002/anie.202405125

Photocatalysis

Photoredox-Catalyzed Decarboxylation of Oxetane-2-Carboxylic Acids and Unique Mechanistic Insights

*Elvis C. McFee, Katie A. Rykaczewski, and Corinna S. Schindler**

Abstract: Oxetanes are valuable motifs in medicinal chemistry applications, with demonstrated potential to serve as bioisosteres for an array of functional groups. Through the visible-light-mediated photoredox hydrodecarboxylation of 2-aryl oxetane 2-carboxylic acids this work enables access to the products of a [2+2]-photocycloaddition between alkenes and aryl aldehydes without the challenges associated with a traditional UV-light-mediated Paternò-Büchi reaction. Investigation into the hydrodecarboxylation mechanism reveals substrate-dependent modes of initiation under the conditions reported herein. Divergence in diastereomeric outcome is observed, with mechanistic probes elucidating key hydrogen-bonding and steric interactions.

Introduction

Oxetanes (**1**), with unique structural features, are crucial in pharmaceutical research as bioisosteres for carbonyls and gem-dimethyl groups.[1] Recent advancements in oxetane functionalization have showcased innovative strategies centered around radical generation in the 3-position, leveraging a variety of functional handles such as aldehydes,[1d] alkenes,[2] silanes,[3] and sulfonyl fluorides.[4] Notably, the incorporation of carboxylic acids at the oxetane 3-position (**2**) has emerged as a particularly valuable technique, enabling the generation of diverse oxetane building blocks through radical pathways (Figure 1A).[5] While functionalizing oxetanes at the 2-position is equally desirable, this area remains relatively unexplored, likely due to challenges linked to the stability of the resulting α-oxy-radicals (**4**, vida infra).[5a] Notable approaches using C–H activation by Ravelli,[6] MacMillan,[7] and photoredox decarboxylation by Sherwood,[8] have led to intermediate α-oxy oxetane radicals (**4**). Despite these advances, photoredox decarboxylation strategies to facilitate functionalization in the 2-position of densely substituted oxetanes have yet to be developed, presenting a significant opportunity for future research and innovation.[9]

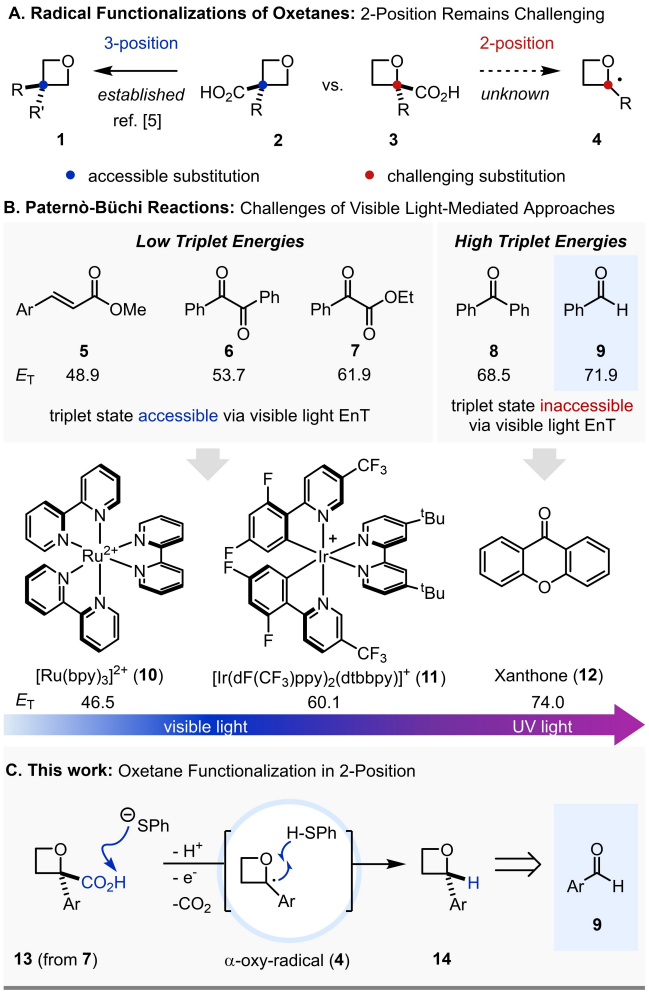


Figure 1. **A.** Decarboxylative functionalization of 3-oxetane carboxylic acids (2) is well established,[5] while examples of decarboxylative functionalization at 2- and 4- positions are underexplored. **B.** The visible-light-enabled triplet energy transfer (EnT) Paternò–Büchi reaction is limited to carbonyls with lower triplet energy (E_T). Triplet excited state energies expressed in kcal/mol.[11] **C.** This work demonstrates that aryl glyoxylates (**7**) can serve as synthons for aryl aldehydes (**9**), enabling the synthesis of 2-aryl oxetanes (**14**) via visible light photocatalysis.

An efficient method to access densely substituted oxetane precursors bearing carboxylate substitution at the 2-position is the Paternò-Büchi reaction, which proceeds via a [2+2]-photocycloaddition between carbonyls and alkenes. Recent approaches have utilized visible-light-enabled triplet energy transfer (EnT) to facilitate the Paternò-Büchi

[*] E. C. McFee, K. A. Rykaczewski, Prof. C. S. Schindler
Department of Chemistry
University of Michigan
930 North University Avenue, Ann Arbor, Michigan 48109, United States
E-mail: corinnas@umich.edu

© 2024 Wiley-VCH GmbH

reaction, offering enhanced functional group compatibility and eliminating the need for UV-light.[10] Yet, the accessibility of oxetanes by this method hinges on pairing the corresponding carbonyl with a photocatalyst of sufficiently high triplet energy (ET) (Figure 1B). While the visible-light-mediated EnT Paternò-Büchi reaction enables the synthesis of 2-aryloxetane-2-carboxylates (**13**) from aryl glyoxylates (**7**), many carbonyls (i.e. aryl aldehydes **9**, ET = 68.5 kcal/mol) have triplet energies surpassing those of state-of-the-art visible light-absorbing photocatalysts (i.e. **11**, 60.1 kcal/mol).[11a,15] Thus, for carbonyls such as aryl aldehydes (**9**) to engage in the Paternò-Büchi, direct excitation using UV-light is typically required.

We envision a visible-light-mediated strategy utilizing aryl glyoxylates (**7**) to form 2-aryloxetane-2-carboxylates (**13**), followed by subsequent decarboxylation to access 2-aryloxetanes (**14**). By utilizing this strategy one can now access the products of a net [2+2]-photocycloaddition between aryl aldehydes and alkenes—a transformation that, depending on the alkene component, can be very limited under UV-light conditions (*vida infra*).

Importantly, the development of this strategy provides the opportunity to explore the reactivity of the key α-oxy radical intermediate (**4**), uncovering the challenges related to overoxidation to the oxocarbenium that must be overcome. Further investigation into the hydrodecarboxylation mechanism suggests two distinct initiation pathways that have not previously been proposed (i.e. pathways that arise under low polarity and weakly basic conditions).

Results and Discussion

The main challenge to oxidative decarboxylation strategies centers on the unstable nature of benzylic α-oxy radical intermediates (**22a**, **22b**) which are prone to overoxidation to an oxocarbenium intermediate and subsequent ring-opening. This challenge is highlighted by the deleterious reactivity of oxetane-2-carboxylic acid **16** and *N*-hydroxyphthalimide (NHPI) ester **17** under typical decarboxylative conditions (Figure 2A). Treatment of carboxylic acid **16** with catalytic silver and a stoichiometric terminal oxidant ($AgNO_3/K_2S_2O_8$) yielded ring-opened β-keto-alcohol **18** in 54 % yield (Figure 1B).[12] Similarly, photocatalytic reduction of NHPI ester **17** using a PPh_3/NaI charge transfer complex produced the ring-opened β-iodo-ketone **19** (12 % yield).[13] Furthermore, activation of NHPI ester **17** under photoredox (*fac*-Ir(ppy)$_3$) resulted in the formation of the ring-opened β-ketoaldehyde **20** (29 % yield).[14] These results underscore the challenges highlighted above, namely, overoxidation of α-oxy-radical intermediates (**22a**, **22b**) followed by undesired nucleophilic attack or ring-opening (Figure 1C).

These results indicate that mitigating the oxidation of the benzylic α-oxy-radical (**22a**) to the corresponding cation (**23a**) represents a key challenge in intercepting oxetane radical (**22a**) to form 2-aryloxetane products (**24**). In contrast to phthalimide esters (**17**), we hypothesized that photoredox decarboxylation of oxetane carboxylates (**21**$^-$) would proceed through a reductive quenching cycle, generating the α-oxy-radical (**22a**) alongside the reduced state of the photocatalyst. This minimizes the probability of a second oxidation and increases the likelihood of productive

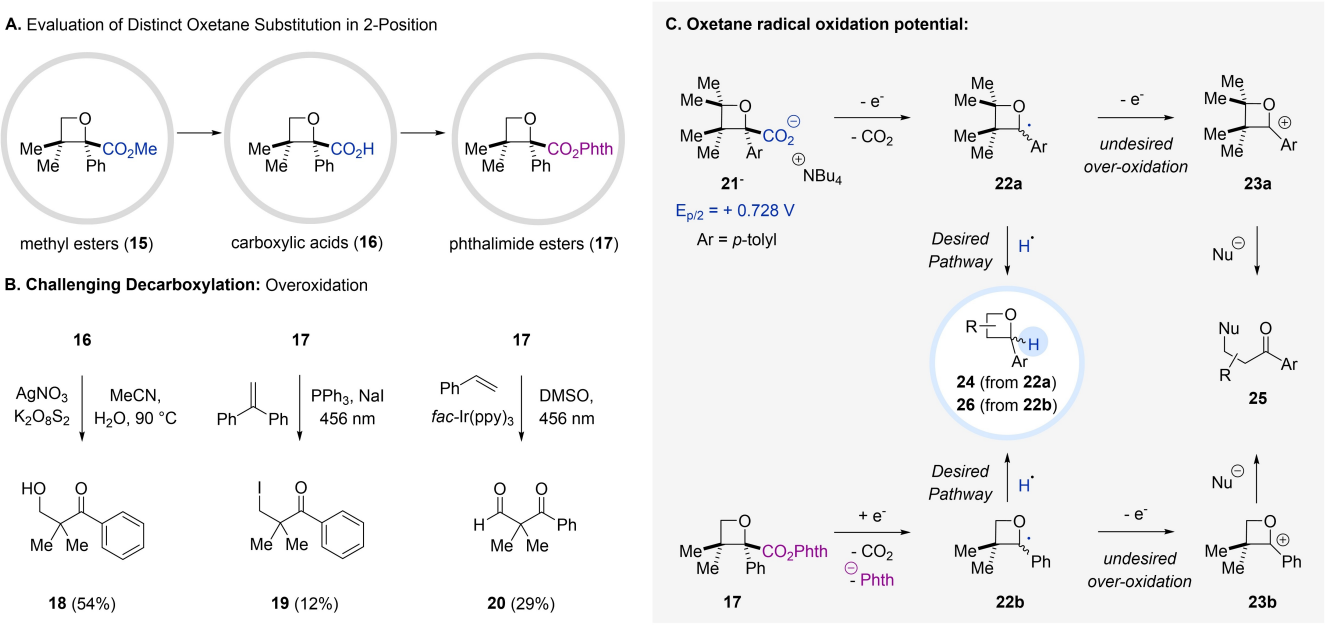


Figure 2. **A**. Initial oxetane substrates evaluated in decarboxylative functionalization reactions were carboxylic acid **16** and NHPI ester **17**, both accessible from methyl ester oxetane **15**. **B**. Reaction conditions that led to the over-oxidation of carboxylic acid **16** to form **18**,[12] and the over-oxidation of NHPI ester **17** to form **19**[13] and **20**.[14] Yields determined via ^{1}H NMR with mesitylene as internal standard. **C**. Oxidation potential (vs. SCE) of **22a** occurs at a lower potential than **21**$^-$, likely giving oxo-carbenium **23a** which can undergo ring opening to give SN2 products (**25**).

© 2024 Wiley-VCH GmbH

reactivity of oxetane α-oxy-radical intermediate (**22a**). Photoredox decarboxylation of oxetane-2-carboxylic acids (**16**) was considered to hold the highest potential for success due to the inherent low steady-state concentration of oxidizing catalyst species.

Based on this hypothesis, the photoredox decarboxylation of acid **16** was explored (Table 1). Approaches utilizing hydrogen atom transfer from transiently generated thiophenol to quench the intermediate α-oxy-radical showed the most promise.[16]

Optimization of the initial conditions revealed that neutral organic photocatalysts exhibited limited reactivity (0–12 %; Table 1, entries 2–3).[18] To our surprise, $Ru(bpy)_3^{2+}$ showed no reactivity (Table 1, entry 4). However, further investigation reveals a correlation between base pKa and carboxylic acid oxidation potential, suggesting that **16** in the presence of DIPEA requires a photocatalyst with a higher excited state reduction potential (see $E_{p/2}$ vs. pKa plot in Supporting Information for details). Cationic photocatalysts with higher excited-state reduction potentials (**28**, **11**) resulted in the desired hydrodecarboxylation product **26** with improved yields of up to 65 % (Table 1, entries 5–6).

Acridinium-based photocatalysts (**28**) resulted in optimal yields in trifluoroethanol (TFE), in-line with previous reports.[16a] Iridium-based photocatalyst **11** exhibited the highest yields of 65 % in ethyl acetate (Table 1, entry 6). A comparison of these conditions revealed that the iridium photocatalyst **11** in ethyl acetate generally provided higher yields across various substrates, leading to its selection as the optimal photocatalyst for this transformation (see Supporting Information for details). Notably, under conditions utilizing photocatalyst **11**, the reaction was low yielding in H-bonding solvents such as MeOH (<5 %) and TFE (0 %), while moderate yields were observed in acetonitrile (20 %), toluene (52 %), and trifluorotoluene (36 %) (Table 1, entry 7). Further evaluation of the reaction showed that exclusion of any reaction component resulted in no product formation (Table 1, entries 8–11).

The lack of reactivity when using photocatalyst **11** in TFE was striking and may be the result of changes in electronic properties of the substrate and photocatalyst in the strong hydrogen-bonding environment, similar to what has been described previously.[19]

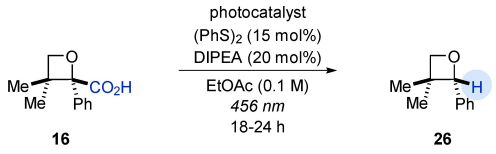
Having identified optimal reaction conditions for the hydrodecarboxylation of oxetanes, the scope of this transformation was explored (Scheme 1). It was observed that 2-aryloxetane-2-carboxylic acids bearing an electron-rich arene provided products **32** and **24** in good yields (88 % and 89 %, respectively). In comparison, 2-aryloxetane-2-carboxylic acids with electron-withdrawing groups on the arene gave slightly lower yields of products **30** (74 %) and **31** (69 %). Substrates with fewer substituents at the 4-position performed comparably, yielding products **35** (75 %, 1.1:1 d.r., 7.4:1 r.r.) and **36** (62 %).

Fused bicyclic oxetanes also successfully underwent the transformation, yielding products **34** (61 %) and **41** (35 %) as single diastereomers. The reaction exhibited tolerance to electron-rich arenes at the 3-position, producing products **37** (78 %, 2.8:1 d.r.) and **38** (42 %, 3.0:1 d.r.). Oxetane-2-carboxylic acids with a *t*-butyl ether at the 3-position were also well-tolerated, providing products **39** (53 %, 1.7:1 d.r.) and **40** (71 %, 1.7:1 d.r.).

A noteworthy distinction of this methodology is its ability to access oxetanes that are not accessible under traditional UV-light Paternò-Büchi reaction conditions. While a direct [2+2]-photocycloaddition between *p*-tolualdehyde and 2,3-dimethylbutene was able to afford oxetane product **24** in 61 % yield, oxetane products derived from conjugated alkenes (**34**, **37**) were only produced in trace yield under the UV-light-mediated approach. These reactions suffered from competing excitation of the alkene, as indicated by the predominant *cis-trans* isomerization of *trans*-anethole and dimerization of indene. This highlights the synthetic value of utilizing aryl glyoxylic acids as aryl aldehyde synthons.

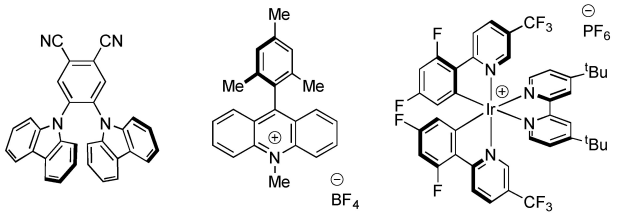
During the investigation of the substrate scope, we noticed distinct diastereoselectivity differences between 2,3-diaryl oxetanes (**42**) and 3-ether-2-aryloxetanes (**43**), which favor the formation of the *syn*-diastereomer **37a** or *anti*-

Table 1: Hydrodecarboxylation of Oxetane-2-Carboxylic Acids.[a]



16 **26**

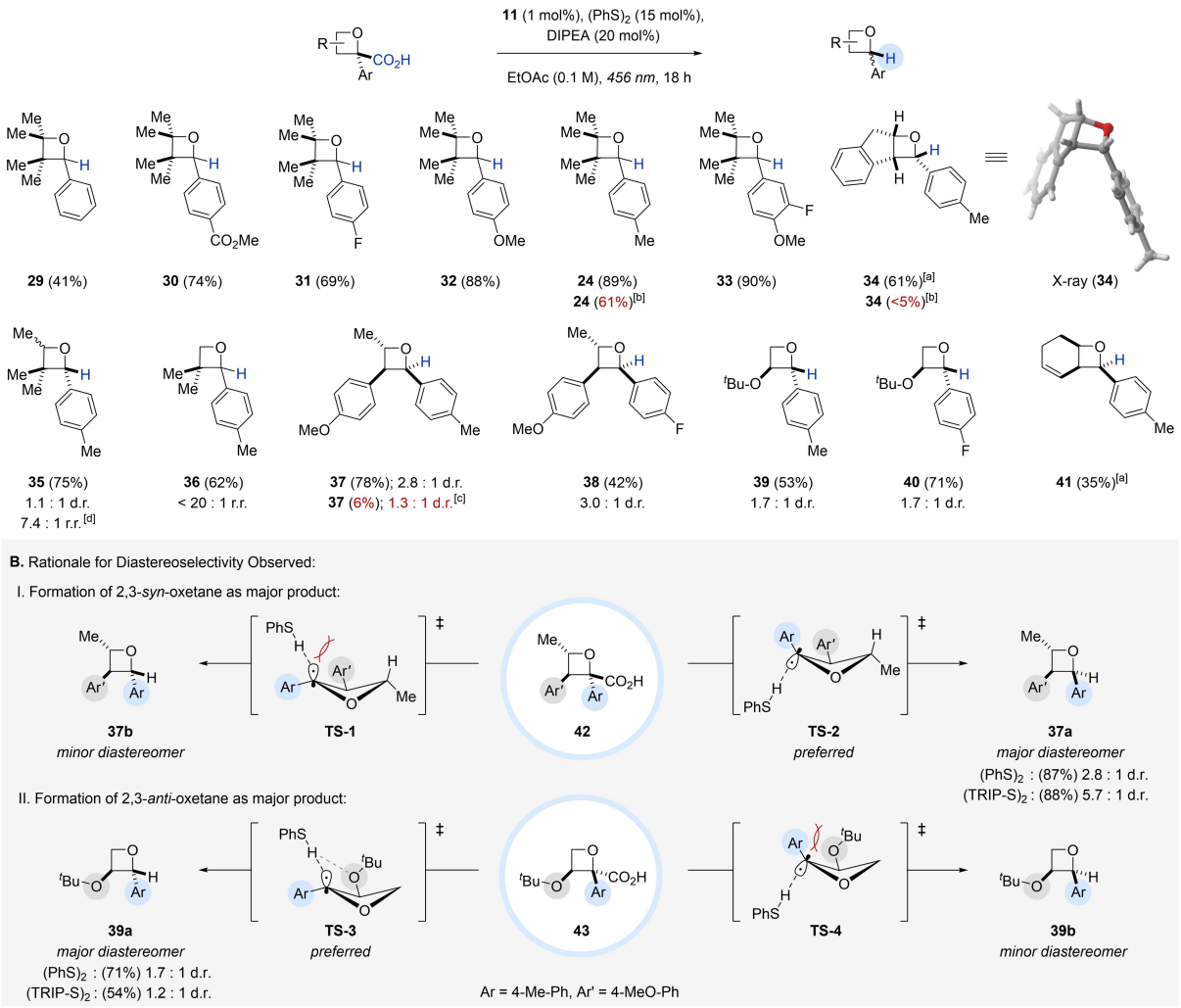
entry	catalyst	$E_{1/2}(PC^*/PC^-)$	$E_{1/2}(PC/PC^-)$	yield (%)	**16** (%)
1	*fac*-Ir(*p*-CF_3-ppy)$_3$	0.59	-2.18	4	63
2	2CzPN	1.32	-1.45	12	43
3	3CzClIPN	1.56	-1.16	<5	76
4	$[Ru(bpy)_3](PF_6)_2$	0.77	-1.33	<5	83
5[b]	[Mes-Acr-Me](BF_4)	2.08	-0.57	48	<5
6	**11**	1.21	-1.37	65	<5%
	deviation from above conditions				
7	Other Solvent (MeOH, MeCN, PhMe, or TFE)			0–52	
8	No photocatalyst			0	
9	**11**, no $(PhS)_2$			0	
10	**11**, no base			0	
11	**11** no hν, 40 °C			0	



2CzPN (**27**) Mes-Acr-Me$^+BF_4^-$ (**28**) $[Ir(dF(CF_3)ppy)_2(dtbbpy)]PF_6$ (**11**)

[a] All reactions were performed using 0.1 mmol of substrate at 0.1 M concentration. $[Ir(dF(CF_3)ppy)_2(dtbbpy)]PF_6$ (**11**) used in 1 mol % and all other photocatalyst used in 3 mol %. Reactions irradiated with two kessil 456 nm lamps. Yields determined via ^1H NMR, using mesitylene as internal standard. Photocatalysts redox potentials taken from the literature.[15,17] No major ring-opened products identified in all cases. [b] Yields represent an average of two or more reactions.

© 2024 Wiley-VCH GmbH



Scheme 1. A. Substrate scope of the hydrodecarboxylation of oxetane-2-carboxylic acids. **Reaction Conditions**: Reactions were performed on oxetane carboxylic acid substrates (0.1 mmol) in ethyl acetate (0.1 M) with photocatalysts **11** (1 mol%), $(PhS)_2$ (15 mol%), and DIPEA (20 mol%) with blue light irradiation (456 nm) for 18 hours. Reactions maintained at 30–35 °C with fan cooling. Yields of isolated products shown in parentheses. Reported diastereomeric ratios obtained from ^{1}H NMR analysis of the crude reaction mixtures. [a] Product formed as a single diastereomer. [b] UV-light Paternò–Büchi reaction between p-tolualdehyde (0.1 mmol, 1 equiv.) and respective alkene (0.2 mmol, 2 equiv.) in acetonitrile (0.1 M), yield and d.r. determined via ^{1}H NMR, using Kessil 370 nm lamps, or [c] RPR-3000 A lamps. [d] minor regioisomer results from the Paternò–Büchi to form the substrate. **B**. Proposed rational for the observed diastereomeric outcome of the transformation. Yields and d.r. determined by ^{1}H NMR.

diastereomer **39a**, respectively (Scheme 1B). A possible explanation for the observed selectivity is that the 3-aryl substituent in 2,3-diaryloxetanes (**42**) hinders the approach of thiophenol (**TS-1**), ultimately resulting in preferential delivery of the hydrogen atom to the opposite face (Scheme 1B, I). Additionally, there may be a favorable π–π interaction between arenes that promotes formation of the syn-product. In comparison, selectivity observed from substrates bearing a pendant ether at the 3-position (**43**) could be driven by a hydrogen-bonding interaction between thiophenol and the Lewis basic ether, resulting in predominant delivery of the hydrogen atom from the same face (Scheme 1B, II). To test this hypothesis, we conducted the hydrodecarboxylation reaction of oxetanes **42** and **43** relying on $(TRIP–S)_2$ as a sterically encumbered aryl thiol precursor. Notably, under conditions utilizing $(TRIP–S)_2$, 2,3-diaryloxetane-2-carboxylic acid **42** showed improved selectivity in forming the *syn*-product **37a** (88%, 5.7:1 d.r.). This outcome supports the proposed rationale for diastereoselectivity for 2,3-diaryloxetanes, as increased steric bulk on the aryl thiol is expected to further increase the energy barrier of the less-preferred transition state **TS-1**. In comparison, 3-(*tert*-butoxy)-2-aryloxetane-2-carboxylic acid **43** resulted in diminished selectivity in forming the *anti*-product **39a** (54%, 1.2:1 d.r.). This is also consistent with our hypothesis, as the increased steric bulk would hinder the hydrogen-bonding interaction between the thiol and Lewis basic ether, increasing the energy barrier of the preferred transition state **TS-3**.

To broaden the synthetic utility of our hydrodecarboxylation approach leveraging aryl glyoxylic acids as aryl aldehyde synthons, we developed a one-pot procedure

© 2024 Wiley-VCH GmbH

combining the initial [2+2]-cycloaddition and subsequent hydrodecarboxylation of the resulting oxetanes (Figure 3). Specifically, glyoxylic acid **44** can undergo the Paternò-Büchi reaction via direct excitation of the carbonyl to form oxetane-2-carboxylic acid **45** in situ. Subsequent conversion under the optimal conditions reported herein for hydrodecarboxylation results in the formation of the desired 2-aryl oxetane **36** in 48 % yield (8.3 : 1.0 r.r.) over 2 steps.

As a result of the low polarity of the optimal solvent used herein, it was deemed worthwhile to investigate the possible mechanistic implications, specifically with regards to changes in the nature of the acid-base interaction. Previous detailed mechanistic investigations into photoredox hydrodecarboxylation by the Nicewicz group proposed that the excited state of the photocatalyst is quenched by a discrete carboxylate, formed upon deprotonation of the carboxylic acid substrate by DIPEA in polar protic solvents (i.e. TFE).[16a] In their case, the high polarity of the solvent likely pushes the acid-base equilibrium towards near-complete formation of the protonated ammonium and carboxylate species. As a result of this, the likelihood of DIPEA quenching the excited-state of the photocatalyst to form an aminium radical cation was nullified therein.

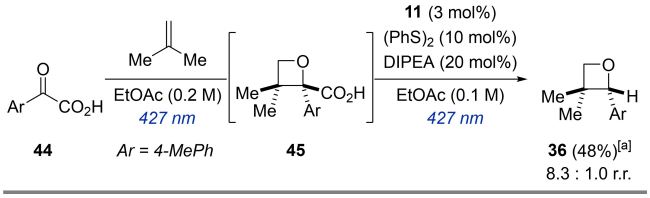


Figure 3. Sequential 2-step, 1-pot synthesis of hydrodecarboxylated oxetane **36** from aryl glyoxylic acid **44**. Photocatalyst **11** added after completion of the first step. [a] Isolated yield over 2 steps.

However, the reaction conditions herein rely on ethyl acetate for optimal performance, and the likelihood of full deprotonation to a discrete carboxylate species is less probable. Therefore, the redox innocence of DIPEA is brought into question. Looking deeper into this possible deviation in mechanism, the nature of the acid-base interaction was first probed via ^{1}H NMR titration of **16** with DIPEA. As the concentration of DIPEA was increased, the change in arene proton resonance of oxetane acid **16** was measured. This change in ^{1}H NMR proton resonance was plotted versus [DIPEA]/[**16**] and subjected to non-linear fitting (Figure 4A) (see Supporting Information for details).[20] This fitting revealed a plateau in arene ^{1}H resonance change ($\delta = 7.73$ ppm) which falls short of the carboxylate measured independently in the same solvent ($\delta = 7.82$ ppm). This data reveals that a hydrogen-bonding complex (with an equilibrium constant of $K_{eq} = 288.5\ M^{-1}$) is more likely than the formation of a discrete carboxylate species. Through this equilibrium constant it is revealed that under the initial reaction conditions, approximately 96 % of the DIPEA forms **16**·DIPEA, with only 4 % free DIPEA that could undergo oxidation by the photocatalyst (Figure 4B).

The relative rates of photocatalyst quenching by **16**·DIPEA and free DIPEA were determined through a series of Stern–Volmer quenching studies.[21] First, the Stern–Volmer quenching constants of DIPEA and **16** were independently measured, revealing negligible quenching from **16** alone and a DIPEA quenching constant of $K_{SV(DIPEA)} = 4034\ M^{-1}$ (Figure 4C, i.; see Supporting Information for details). The quenching of a mixture of DIPEA and **16** was then

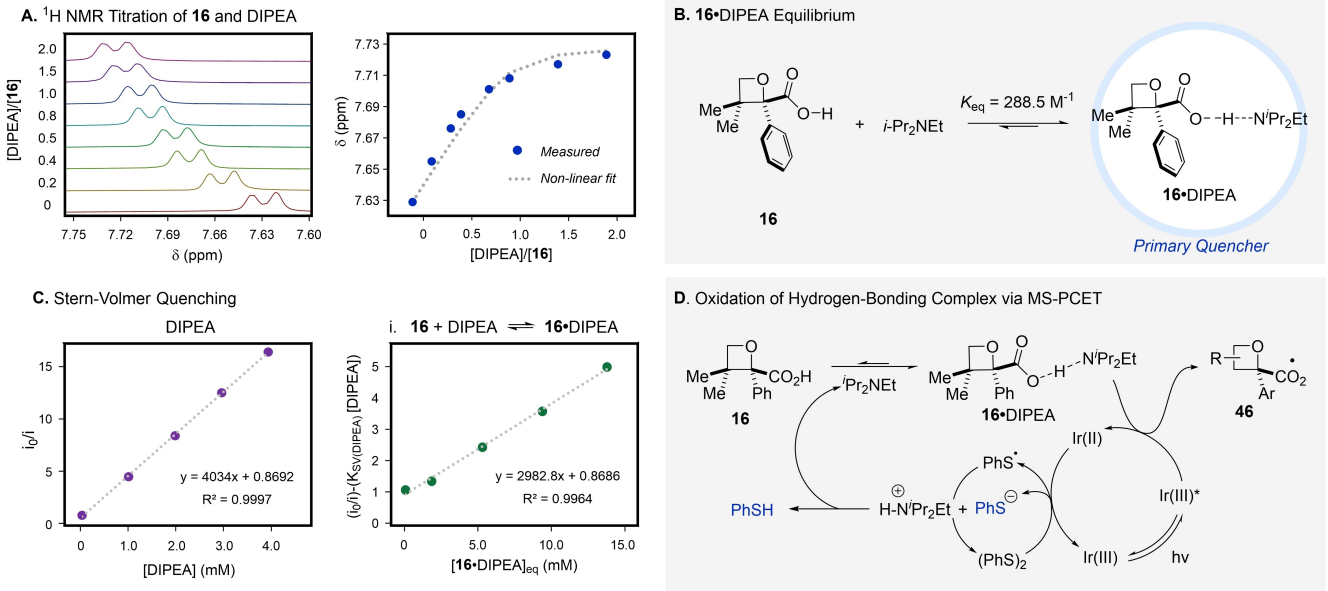


Figure 4. The equilibrium association constant for the formation of **16**·DIPEA was determined by ^{1}H NMR in titration of **16** and DIPEA. **B.** The equilibrium association constant reveals that under the initial reaction conditions $[DIPEA]_{eq}$ is much lower than $[\mathbf{16}\cdot DIPEA]_{eq}$. **C.** Stern–Volmer Quenching measurements of **i.** DIPEA alone, and **ii.** $[\mathbf{16}\cdot DIPEA]_{eq}$. **D.** Proposed mechanism for oxidation of **16**·DIPEA via MS-CPET.

© 2024 Wiley-VCH GmbH

measured, and the H-bonding association constant K_{eq} was used to determine the equilibrium concentrations of **16**·DIPEA and free DIPEA. By subtracting the quenching contribution of DIPEA from the total quenching observed for the mixture, the Stern–Volmer quenching constant of **16**·DIPEA was determined to be $K_{SV(\mathbf{16}\cdot DIPEA)} = 2982.8\ M^{-1}$ (Figure 4C, ii.; see Supporting Information for details). This indicates that, under the initial reaction concentrations, approximately 95 % of the excited state photocatalyst is quenched by **16**·DIPEA.

This quenching is proposed to occur via a multiple-site concerted proton electron transfer (MS-CPET) to generate the carboxyl radical and the protonated ammonium species (Figure 4D).[22] The generated Ir(II) can then reduce $(PhS)_2$ ($E^0 = -1.12$ V vs. SCE)[23] to regenerate the ground-state Ir(III). The generated thiophenolate will readily deprotonate the ammonium, forming thiophenol and regenerating DIPEA (Figure 4D), enabling use of catalytic DIPEA. This proton transfer from protonated DIPEA to thiophenolate is supported by ^{1}H NMR titration of thiophenol with DIPEA (see Supporting Information for details).

However, upon repeating the same analysis sequence for a more sterically encumbered substrate (**21**), further deviation from the previously reported hydrodecarboxylation mechanism was revealed.[16a] Similar to oxetane-2-carboxylic acid **16**, fully-substituted oxetane-2-carboxylic acid **21** was found to form H-bonding complex **21**·DIPEA, albeit with a lower association constant of $K_{eq(\mathbf{21}\cdot DIPEA)} = 76.3\ M^{-1}$ (Figure 5A, 5B).

Furthermore, the Stern–Volmer quenching studies of a mixture of DIPEA and **21** found that all observed quenching can be attributed to free DIPEA at equilibrium (Figure 5C; see Supporting Information for details). Therefore, it is imperative that a mechanism involving the sacrificial oxidation of DIPEA be considered for our system.[24]

A previous report of a photoredox transformation utilizing a substoichiometric trialkylamine as a redox mediator has been reported by Gilmour, where the generated aminium radical was proposed to facilitate an oxidation.[25] Such a mechanism was considered here, where the aminium radical cation might be capable of oxidizing the oxetane carboxylate **21**$^-$. However, based on independent oxidation potential measurements of DIPEA ($E_{p/2} = 0.65$ V vs. SCE) and carboxylate **21**$^-$ ($E_{p/2} = 0.73$ V vs. SCE), such a possibility was considered unlikely.

All things considered, we propose that for bulkier substrates (**21**), the primary role of DIPEA is in the reaction initiation, serving as a sacrificial reductant to reduce the excited-state Ir(III)*. The generated Ir(II) then reduces $(PhS)_2$ to regenerate the ground-state Ir(III). Following fragmentation, the generated thiophenolate then deprotonates the carboxylic acid (**21**) to give carboxylate (**21**$^-$) and thiophenol (Figure 5D).

Following either mode of initiation discussed above, the mechanism is proposed to follow the same termination steps for **21**$^-$ and **16**·DIPEA. The excited-state photocatalyst drives the oxidation to form carboxyl radical **46** via single electron oxidation from the carboxylate (**21**$^-$), or by MS-CPET oxidation of the H-bonding complex (**16**·DIPEA). Extrusion of CO_2 from carboxyl radical **46** generates the key oxetane radical intermediate **47**, which is subsequently quenched by thiophenol via hydrogen-atom transfer to give the hydrodecarboxylated oxetane product (**48**) (Figure 6).

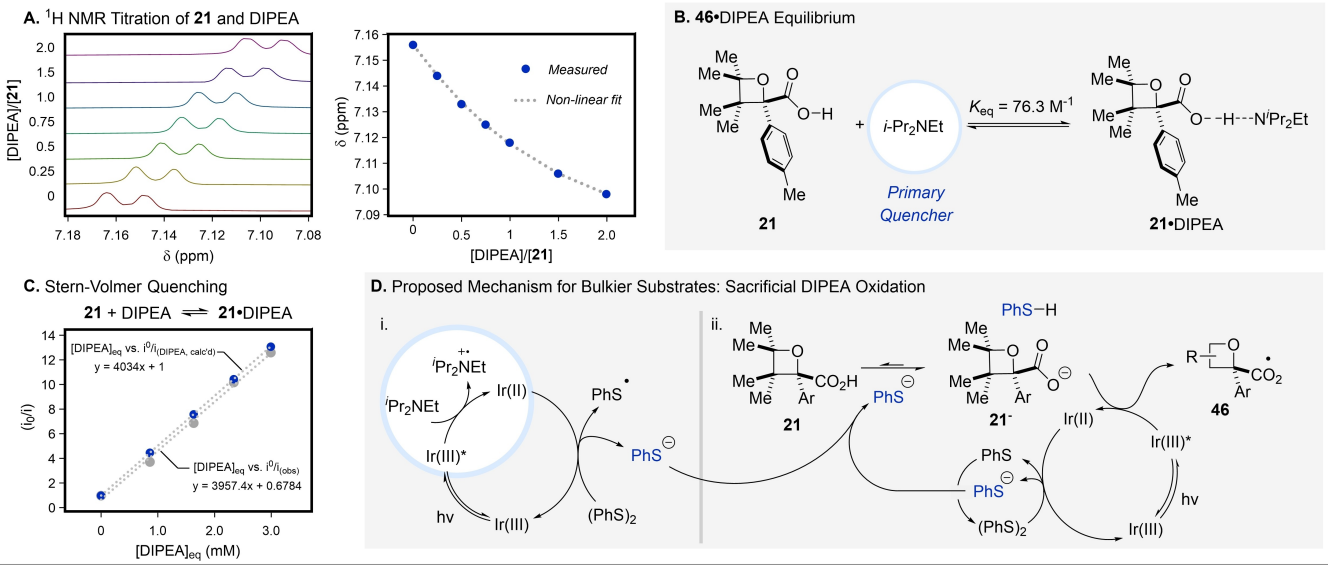


Figure 5. **A**. The equilibrium association constant for the formation of **21**·DIPEA was determined by ^{1}H NMR in titration of **16** and DIPEA. **B**. The equilibrium association for the formation of **21**·DIPEA. **C**. Stern–Volmer Quenching of **21** and DIPEA in equilibrium, revealing that all observed quenching can be attributed to DIPEA alone. **D. i**. Proposed initiation mechanism, where DIPEA is oxidized sacrificially to enable the formation of phenylthiolate. **ii**. The deprotonation of **21** and subsequent oxidation of 21$^-$.

© 2024 Wiley-VCH GmbH

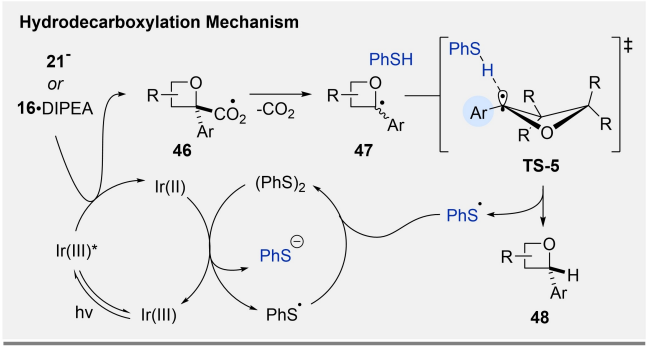


Figure 6. General mechanism for the hydrodecarboxylation of oxetanes following the formation of **21**$^-$ or **16**·DIPEA.

Conclusions

In summary, a key challenge in the decarboxylation of oxetane-2-carboxylic acids (**16**) and its phthalimide ester derivatives (**17**) is the undesirable oxidation of the intermediate radical (**22a**) and the subsequent formation of nucleophilic ring opening products (**25**). This challenge can be overcome efficiently by relying on photoredox catalysis, specifically utilizing a reductive photoredox quenching cycle for the oxidation of the carboxylate (**21**$^-$) and rapid capture of the resulting oxetane radical (**22**). The products accessible are formally the result of a net [2+2]-cycloaddition between alkenes and aryl aldehydes that requires UV-light irradiation and often proves challenging, resulting in low yields. The method described herein establishes a two-step strategy that leverages aryl glyoxylates as synthons for aryl aldehydes and ultimately enables a visible-light-mediated approach to access 2-aryl oxetanes. Our mechanistic investigation into the hydrodecarboxylation reveals two new modes of reaction initiation that are distinct from previous methods, arising from the reaction conditions reported herein. Specifically, the reaction can initiate via oxidation of an H-bonding complex (**16**·DIPEA) through MS-CPET, or by sacrificial oxidation of DIPEA to ultimately generate thiophenolate to act as a stronger base. We suspect that both initiation mechanisms are operative and preference for one over the would be dictated by the steric environment around the carboxylic acid and its acidity.

Supporting Information

The authors have cited additional references within the Supporting Information.[26]

Deposition Numbers CCDC 2333181 and CCDC 2333180 contain the supplementary crystallographic data for **S16** and **34** respectively. These data are provided free of charge by the joint Cambridge Crystallographic Data Centre and Fachinformationszentrum Karlsruhe Access Structures service.

Acknowledgements

This work was supported by the NSF Center for the Chemistry of Molecularly Optimized Networks (MONET; Award CHE2116298). KAR thanks the NSF GRFP for a predoctoral fellowship. We thank L. M. Foroughi for X-ray crystallography services. We thank C. R. J. Stephenson for helpful discussions on mechanistic investigations.

Conflict of Interest

The authors declare no conflict of interest.

Data Availability Statement

The data that support the findings of this study are available in the supplementary material of this article.

Keywords: Oxetane · Photocatalysis · Photoredox · Decarboxylation · Reaction Mechanisms

[1] a) G. Wuitschik, M. Rogers-Evans, K. Muller, H. Fischer, B. Wagner, F. Schuler, L. Polonchuk, E. M. Carreira, *Angew. Chem. Int. Ed.* **2006**, *45*, 7736–7739; b) J. A. Burkhard, G. Wuitschik, M. Rogers-Evans, K. Müller, E. M. Carreira, *Angew. Chem. Int. Ed.* **2010**, *49*, 9052–9067; c) A. F. Stepan, K. Karki, W. S. McDonald, P. H. Dorff, J. K. Dutra, K. J. DiRico, A. Won, C. Subramanyam, I. V. Efremov, C. J. O'Donnell, C. E. Nolan, S. L. Becker, L. R. Pustilnik, B. Sneed, H. Sun, Y. Lu, A. E. Robshaw, D. Riddell, T. J. O'Sullivan, E. Sibley, S. Capetta, K. Atchison, A. J. Hallgren, E. Miller, A. Wood, R. S. Obach, *J. Med. Chem.* **2011**, *54*, 7772–7783; d) J. A. Burkhard, G. Wuitschik, J.-M. Plancher, M. Rogers-Evans, E. M. Carreira, *Org. Lett.* **2013**, *15*, 4312–4315.

[2] S. A. Green, S. Vasquez-Cespedes, R. A. Shenvi, *J. Am. Chem. Soc.* **2018**, *140*, 11317–11324.

[3] Y. Zhang, Y. Zhang, X. Shen, *Chem Catal.* **2021**, *1*, 423–436.

[4] J. J. Rojas, R. A. Croft, A. J. Sterling, E. L. Briggs, D. Antermite, D. C. Schmitt, L. Blagojevic, P. Haycock, A. J. P. White, F. Duarte, C. Choi, J. J. Mousseau, J. A. Bull, *Nat. Chem.* **2022**, *14*, 160–169.

[5] a) J. Genovino, Y. Lian, Y. Zhang, T. O. Hope, A. Juneau, Y. Gagne, G. Ingle, M. Frenette, *Org. Lett.* **2018**, *20*, 3229–3232; b) K. Kolahdouzan, R. Khalaf, J. M. Grandner, Y. Chen, J. A. Terrett, M. P. Huestis, *ACS Catal.* **2019**, *10*, 405–411; c) M. A. J. Dubois, J. J. Rojas, A. J. Sterling, H. C. Broderick, M. A. Smith, A. J. P. White, P. W. Miller, C. Choi, J. J. Mousseau, F. Duarte, J. A. Bull, *J. Org. Chem.* **2023**, *88*, 6476–6488.

[6] D. Ravelli, M. Zoccolillo, M. Mella, M. Fagnoni, *Adv. Synth. Catal.* **2014**, *356*, 2781–2786.

[7] a) J. Jin, D. W. C. MacMillan, *Angew. Chem. Int. Ed.* **2015**, *54*, 1565–1569; b) D. F. Fernandez, M. Gonzalez-Esguevillas, S. Keess, F. Schafer, J. Mohr, A. Shavnya, T. Knauber, D. C. Blakemore, D. W. C. MacMillan, *Org. Lett.* **2023**, *26*, 2702–2707.

[8] J. L. Sloane, A. B. Santos, E. M. Simmons, T. C. Sherwood, *Org. Lett.* **2023**, *25*, 4219–4224.

[9] For examples of polar decarboxylations of oxetanes and azetidenes, see: a) O. A. Davis, J. A. Bull, *Angew. Chem. Int.*

© 2024 Wiley-VCH GmbH

Ed. **2014**, *53*, 14230–14234; b) S. P. Fritz, J. F. Moya, M. G. Unthank, E. M. McGarrigle, V. K. Aggarwal, *Synthesis* **2012**, *44*, 1584–1590.
[10] a) K. A. Rykaczewski, C. S. Schindler, *Org. Lett.* **2020**, *22*, 6516–6519; b) J. Zheng, X. Dong, T. P. Yoon, *Org. Lett.* **2020**, *22*, 6520–6525.
[11] a) W. G. Herkstroeter, A. A. Lamola, G. S. Hammond, *J. Am. Chem. Soc.* **2002**, *86*, 4537–4540; b) M. E. Daub, H. Jung, B. J. Lee, J. Won, M. H. Baik, T. P. Yoon, *J. Am. Chem. Soc.* **2019**, *141*, 9543–9547.
[12] W. E. Fristad, M. A. Fry, J. A. Klang, *J. Org. Chem.* **1983**, *48*, 3575–3577.
[13] M. C. Fu, R. Shang, B. Zhao, B. Wang, Y. Fu, *Science* **2019**, *363*, 1429–1434.
[14] A. Tlahuext-Aca, R. A. Garza-Sanchez, M. Schafer, F. Glorius, *Org. Lett.* **2018**, *20*, 1546–1549.
[15] a) N. A. Romero, D. A. Nicewicz, *Chem. Rev.* **2016**, *116*, 10075–10166; b) J. I. Day, K. Teegardin, J. Weaver, J. Chan, *Org. Process Res. Dev.* **2016**, *20*, 1156–1163.
[16] a) J. D. Griffin, M. A. Zeller, D. A. Nicewicz, *J. Am. Chem. Soc.* **2015**, *137*, 11340–11348; b) C. Cassani, G. Bergonzini, C. J. Wallentin, *Org. Lett.* **2014**, *16*, 4228–4231.
[17] a) J. Luo, J. Zhang, *ACS Catal.* **2016**, *6*, 873–877; b) E. Speckmeier, T. G. Fischer, K. Zeitler, *J. Am. Chem. Soc.* **2018**, *140*, 15353–15365.
[18] K. Masui, H. Nakanotani, C. Adachi, *Org. Electron.* **2013**, *14*, 2721–2726.
[19] a) C. Gonzalez, J. Pincock, *Photochem. Photobiol.* **2006**, *82*, 301–309; b) J. Ma, S. Chen, P. Bellotti, R. Guo, F. Schafer, A. Heusler, X. Zhang, C. Daniliuc, M. K. Brown, K. N. Houk, F. Glorius, *Science* **2021**, *371*, 1338–1345; c) R. Ashizawa, T. Noguchi, *Phys. Chem. Chem. Phys.* **2014**, *16*, 11864–11876.
[20] a) R. S. Macomber, *J. Chem. Educ.* **1992**, *69*, 375–378; b) P. Thordarson, *Chem. Soc. Rev.* **2011**, *40*, 1305–1323.
[21] D. M. Arias-Rotondo, J. K. McCusker, *Chem. Soc. Rev.* **2016**, *45*, 5803–5820.
[22] a) R. Tyburski, T. Liu, S. D. Glover, L. Hammarstrom, *J. Am. Chem. Soc.* **2021**, *143*, 560–576; b) W. D. Morris, J. M. Mayer, *J. Am. Chem. Soc.* **2017**, *139*, 10312–10319.
[23] Q. Zhu, C. Costentin, J. Stubbe, D. G. Nocera, *Chem. Sci.* **2023**, *14*, 6876–6881.
[24] a) C. K. Prier, D. A. Rankic, D. W. MacMillan, *Chem. Rev.* **2013**, *113*, 5322–5363; b) J. M. Narayanam, J. W. Tucker, C. R. Stephenson, *J. Am. Chem. Soc.* **2009**, *131*, 8756–8757; c) M. A. Ischay, M. E. Anzovino, J. Du, T. P. Yoon, *J. Am. Chem. Soc.* **2008**, *130*, 12886–12887.
[25] J. Soika, C. McLaughlin, T. Neveselý, C. G. Daniliuc, J. J. Molloy, R. Gilmour, *ACS Catal.* **2022**, *12*, 10047–10056.
[26] a) Tsinghua University and Nankai University, China. *Internet Bond-energy Databank (pKa and BDE)*, can be found under ibond.nankai.edu.cn, (accessed 1 November 2023); b) S. R. Angle, I. Choi, F. S. Tham, *J. Org. Chem.* **2008**, *73*, 6268–6278; c) T. Bach, F. Vogt, K. Jödicke, J. Schröder, *Synthesis* **2009**; d) P. H. J. Carlsen, T. Katsuki, V. S. Martin, K. B. Sharpless, *J. Org. Chem.* **1981**, *46*, 3936–3938; e) T. J. Coxon, M. Fernandez, J. Barwick-Silk, A. I. McKay, L. E. Britton, A. S. Weller, M. C. Willis, *J. Am. Chem. Soc.* **2017**, *139*, 10142–10149; f) S. Jana, F. Li, C. Empel, D. Verspeek, P. Aseeva, R. M. Koenigs, *Chem. Eur. J.* **2020**, *26*, 2586–2591; g) Z. Lu, T. P. Yoon, *Angew. Chem. Int. Ed.* **2012**, *51*, 10329–10332; h) T. Morack, C. Muck-Lichtenfeld, R. Gilmour, *Angew. Chem. Int. Ed.* **2019**, *58*, 1208–1212; i) R. N. Motz, A. C. Sun, D. Lehnherr, S. Ruccolo, *ACS Org. Inorg. Au* **2023**, *3*, 266–273; j) H. G. Roth, N. A. Romero, D. A. Nicewicz, *Synlett* **2016**, *27*, 714–723; k) J. Scheffer, K. Wang, *Synthesis* **2004**, *112*; l) K. Wadhwa, C. Yang, P. West, K. Deming, S. Chemburkar, R. Reddy, *Synth. Commun.* **2008**, *38*, 4434–4444; m) X. C. Xu, D. N. Wu, Y. X. Liang, M. Yang, H. Y. Yuan, Y. L. Zhao, *J. Org. Chem.* **2022**, *87*, 16604–16616; n) T. F. Headen, C. A. Howard, N. T. Skipper, M. A. Wilkinson, D. T. Bowron, A. K. Soper, *J. Am. Chem. Soc.* **2010**, *132*, 5735–5742; o) R. N. Motz, A. C. Sun, D. Lehnherr, S. Ruccolo, *ACS Org. Inorg. Au* **2023**, *3*, 266–273; p) N. A. Romero, D. A. Nicewicz, *J. Am. Chem. Soc.* **2014**, *136*, 17024–17035; q) S. Tsuzuki, K. Honda, T. Uchimaru, M. Mikami, *J. Chem. Phys.* **2005**, *122*; r) S. Wu, J. Žurauskas, M. Domański, P. S. Hitzfeld, V. Butera, D. J. Scott, J. Rehbein, A. Kumar, E. Thyrhaug, J. Hauer, J. P. Barham, *Org. Chem. Front.* **2021**, *8*, 1132–1142; s) D. Zhang, C. Wu, H. Zhou, Y. Ma, Y. Zhu, *Asian J. Org. Chem.* **2022**, *11*, e202200561; t) J. Zurauskas, S. Bohacova, S. Wu, V. Butera, S. Schmid, M. Domanski, T. Slanina, J. P. Barham, *Angew. Chem. Int. Ed.* **2023**, *62*, e202307550.

Manuscript received: April 2, 2024
Accepted manuscript online: December 13, 2024
Version of record online: January 13, 2025

© 2024 Wiley-VCH GmbH